

Supporting Information

Harel et al. 10.1073/pnas.1208690109

SI Experimental Procedures

FACS Isolation and Microarray Screen. Cells were dispersed using a mixture of 0.1% Trypsin and 0.1% Collagenase D (Roche) diluted in F12 (Gibco). FACS Aria (BD Bioscience) was used to isolate YFP⁺ cells. RNA was purified using QIAzol Lysis Reagent (Qiagen). Because of the small tissue samples, mRNA was amplified (Ambion; Message-Amp kit). Hybridization and detection of the mRNAs were performed on Affymetrix GeneChip mouse expression arrays.

X-Gal Staining, Histology, Immunohistochemistry, and in Situ Hybridization. Antibodies used in the study were as follows: Pax7, MyHC, Pecam1, AP2, and Isl1 (1) and mouse monoclonal antibody (Developmental Studies Hybridoma Bank; 1:5–1:10); MyoD, mouse monoclonal (Santa Cruz; 1:200); Lhx2, Rabbit polyclonal (Santa Cruz; 1:100); phospho-histone H3, mouse monoclonal (Cell Signaling; 1:200). Secondary antibodies used were Cy2-, Cy3-, or Cy5-conjugated anti-mouse or anti-rabbit IgG; Cy3-conjugated anti-mouse IgG1; and Cy5-conjugated anti-mouse IgG2b (Jackson ImmunoResearch; 1:200). Images were obtained with a Nikon 90i florescent microscope with the Image Pro Plus program (Media Cybernetics). Images were assembled using Photoshop CS software (Adobe), PTGui stitching software (<http://www.ptgui.com>), and Canvas (ACD Systems). Percentages given in the text were based on the analysis of greater than or equal to six sections from at least two embryos.

ChIP Assay. The pharyngeal arch tissue was dissected from embryonic day (E) 9.5 mice, cross-linked with 1% (wt/vol) formaldehyde and followed by the addition of glycine to quench

formaldehyde. Tissue was washed with ice-cold PBS and lysed in lysis buffer containing a protease inhibitor mixture (Roche). Lysates were sonicated to yield sheared DNA amplicons averaging less than 500 bp. Pre-clearing was performed with salmon sperm DNA, IgGs from the same origin as the primary antibody, and 45 μ L of either protein A or G-Sepharose. Samples were incubated with the following antibodies: goat anti-Pitx2 (C-16; Santa Cruz Biotechnology) overnight at 4 °C followed by the addition of protein A or G-Sepharose for 1 h at 4 °C. After several washes, the DNA was eluted from the Sepharose beads following incubation overnight at 65 °C with RNase A and proteinase K treatment for 2 h at 45 °C. DNA was purified with QIAquick columns (Qiagen). PCR analysis using SYBR Green was done to evaluate the relative abundance of sequences in input and IP material. Primers used are listed in Table S2. Additional ChIP antibodies were T-box transcription factor 1 (Tbx1) (34-9800; Invitrogen); Pitx2 (C16-sc8748 and H80-sc33147; Santa Cruz); Tcf21 (ab32981; Abcam, and sc15006; Santa Cruz), and IgG control (ab37355; Abcam). All antibodies were used at 5 μ g per ChIP experiment.

Vascular Casting. Pregnant mice at E17.5 were anesthetized by light Isoflurane and one horn of the uterus was surgically exposed. Viable embryos from the uterus were removed and kept in ice-cold PBS. The umbilical artery was exposed by opening the yolk sac and injected with a mixture of PBS and Red Baston's No. 17 Casting Solution for 3–4 min. Embryonic tissues were digested by incubation in 20% (wt/vol) KCl for 24–48 h at room temperature. Casts were examined and photographed on a dissecting microscope.

1. Harel I, et al. (2009) Distinct origins and genetic programs of head muscle satellite cells. *Dev Cell* 16(6):822–832.

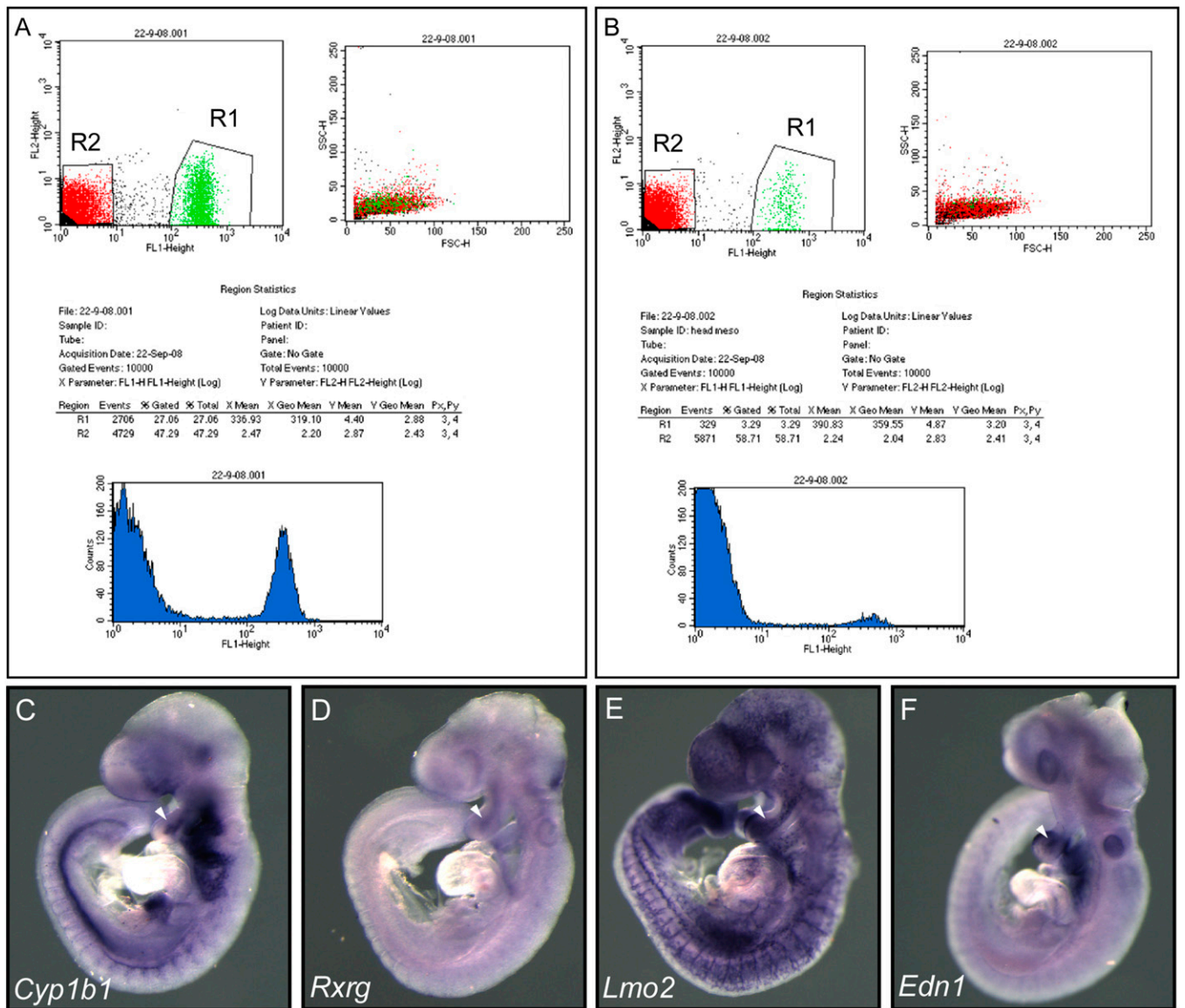


Fig. S1. A screen for pharyngeal mesoderm (PM)-enriched regulators. (A and B) An example of a single FACS isolation procedure, using cells from either interlimb somites (A) or pharyngeal arches (B). Whole-mount in situ hybridization of E9.5 embryos using *Cyp1b1* (C), *Rxrg* (D), *Lmo2* (E), and *Edn1* (F) riboprobes.

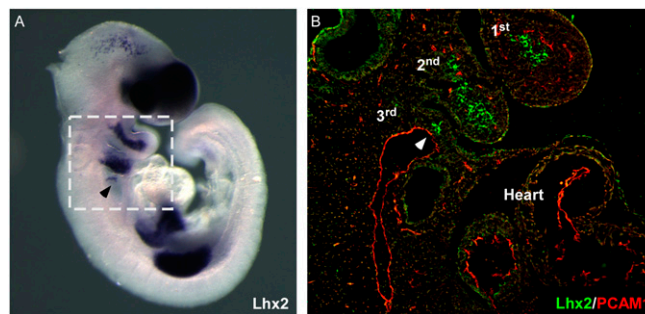


Fig. S2. *Lhx2* is not expressed in PM endothelial cells. (A) Whole-mount in situ hybridization for *Lhx2* at E9.5. (B) *Lhx2* (green) and *Pecam1* (red) staining of the area marked in A. First, second, and third denote the relevant pharyngeal arch.

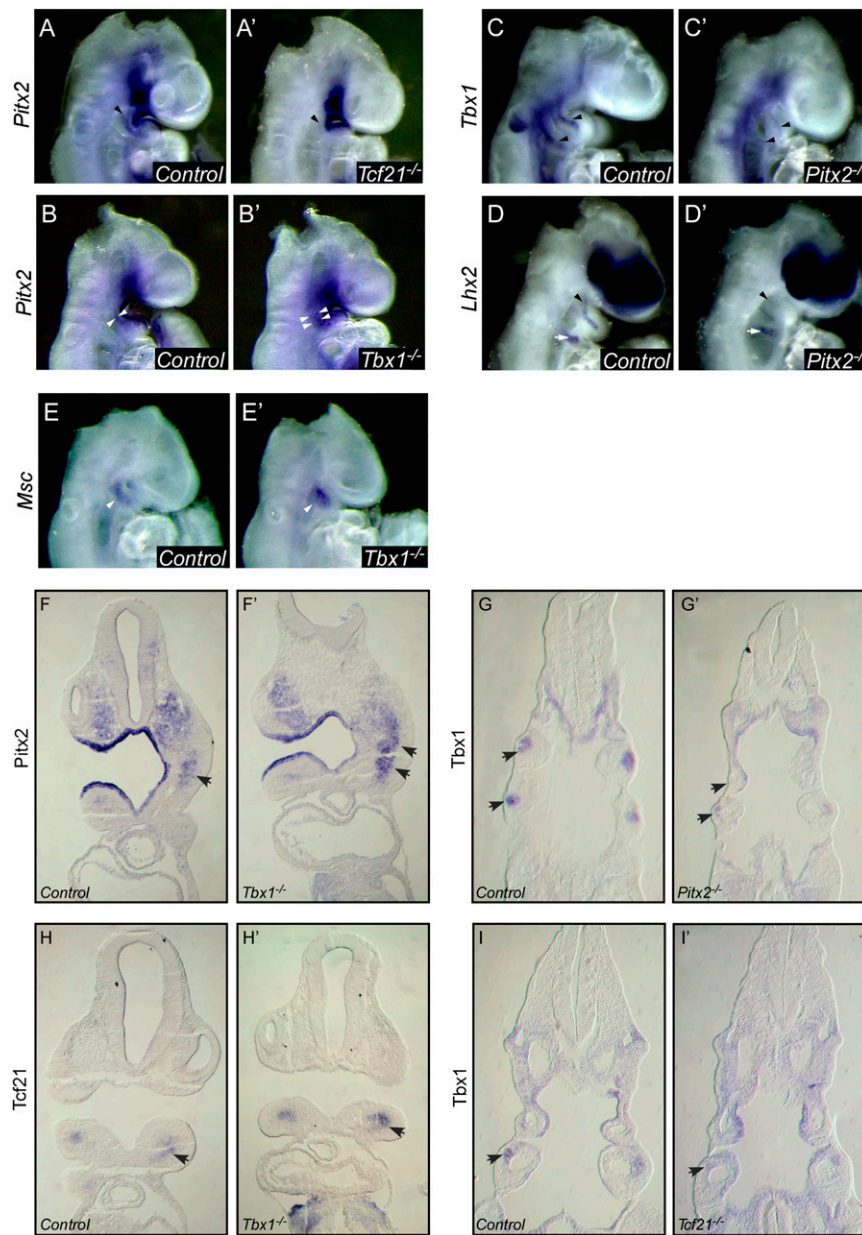
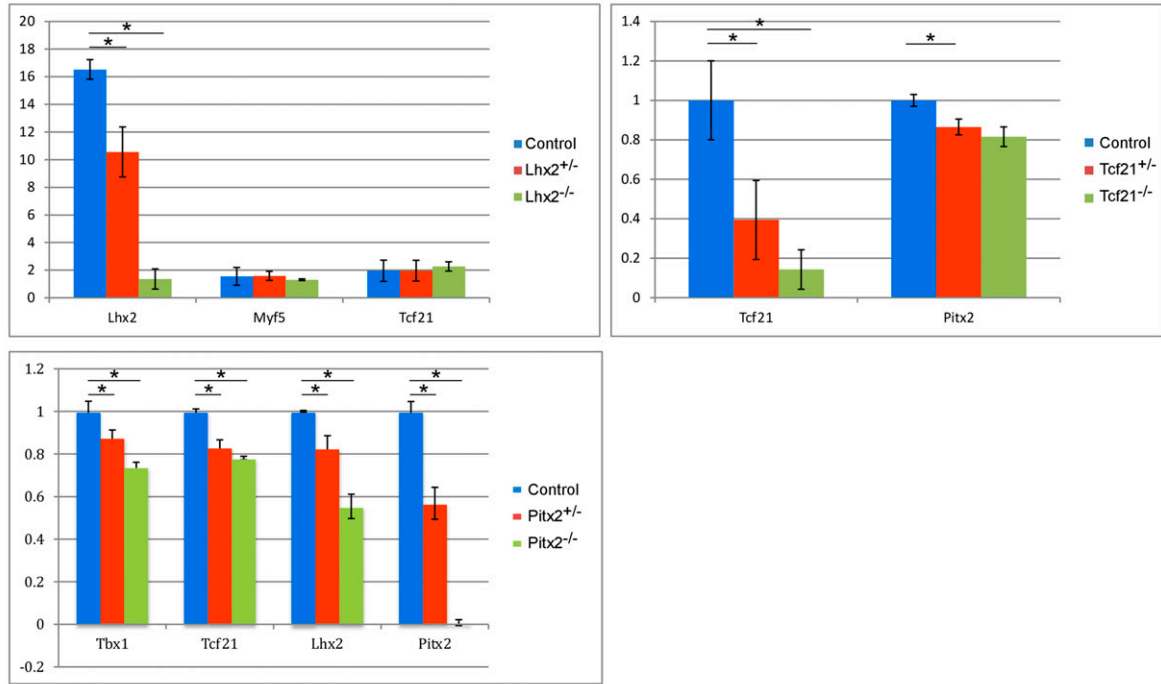
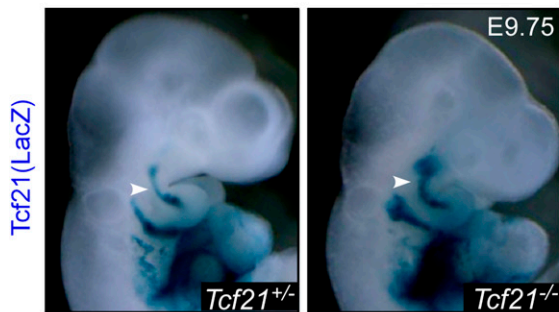


Fig. S3. PM gene expression patterns by in situ sections. (A–E) Whole-mount in situ hybridization for the indicated genes (*Left* of each image) of E9.5 embryos with the indicated genotypes (black rectangles). Arrows/Arrowheads mark the PM: white arrows, unchanged expression; black arrowheads, down-regulated genes; white arrowheads, up-regulated genes. (F–I) Sections for selected embryos, with the indicated genotypes and in situ probes. Arrowheads indicate core of the PM.

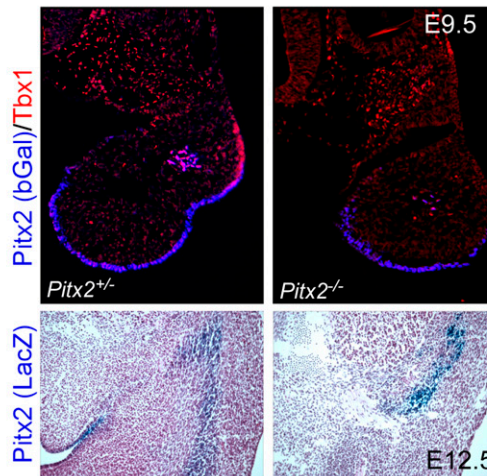
A. qPCR of E9.5 1st-3rd BA



B. Tcf21



Pitx2



C. Pharyngeal muscles

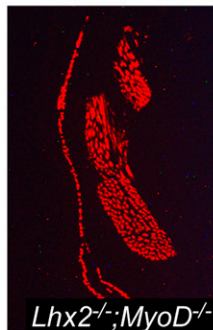
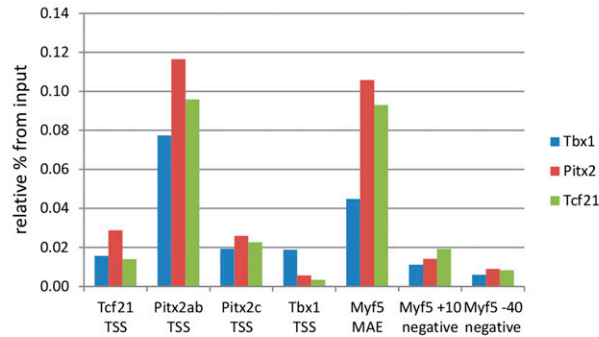
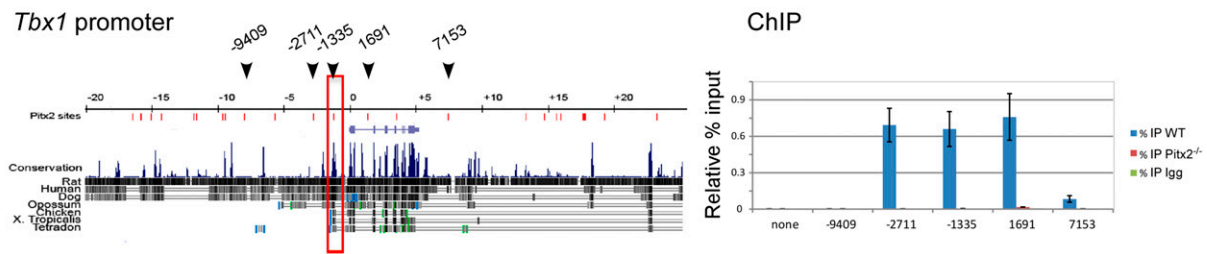


Fig. 54. Evaluation of PM gene expression in *Tcf21*, *Pitx2*, and *Lhx2* mutants. (A) Quantitative RT-PCR (qRT-PCR) for selected PM regulators in *Lhx2*, *Tcf21*, and *Pitx2* mutants, heterozygous and controls. * $P < 0.05$. (B) X-Gal staining of *Tcf21*^{-/-} (*Tcf21*^{LacZ/LacZ}) at E9.75 compared with *Tcf21*^{+/-} controls (Left). Coimmunofluorescence (at E9.5) for Tbx1 and Pitx2 (β-gal), or X-Gal staining (at E12.5), in *Pitx2*^{-/-} and *Pitx2*^{+/-} control embryos (Right). Significant statistical differences ($P < 0.05$) are marked with an asterisk. To test whether PM cells were present in *Tcf21* mutants, we analyzed E9.5 control *Tcf21* (*Tcf21*^{LacZ/+}) and null (*Tcf21*^{LacZ/LacZ}) embryos. X-Gal staining in the mesoderm core of control and *Tcf21* mutants was comparable at E9.5. In line with this result, pharyngeal muscles were not significantly affected in E14 *Tcf21* mutants. We used the same methodology in *Pitx2* control (*Pitx2*^{LacZ/+}) and mutant (*Pitx2*^{LacZ/LacZ}) pharyngeal arches. The mesodermal core, as shown in sections of the first arch stained for Tbx1 and Pitx2 (β-gal) proteins, was reduced in *Pitx2* mutants.

A. ChIP for proximal promoters using Tbx1, Pitx2 and Tcf21 antibodies:



B. Pitx2 binds additional sites on *Tbx1* promoter:

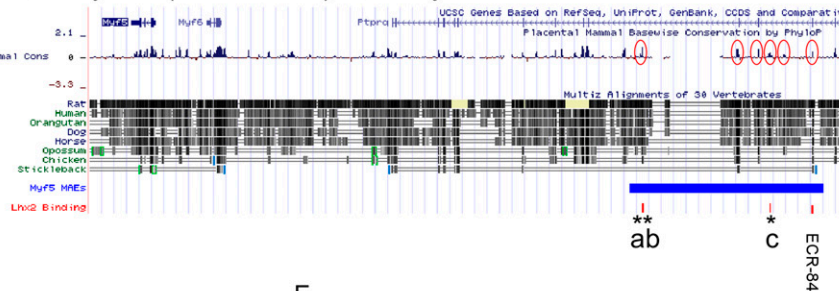


C. Lhx2 binding sites on *Myf5* promoter (Mandibular arch enhancer in Blue):

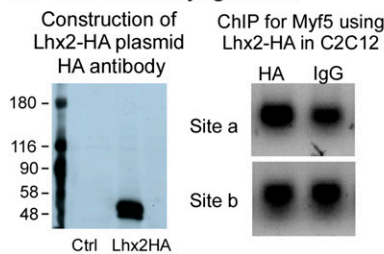
UCSC Genome Browser on Mouse July 2007 (NCBI37/mm9) Assembly

Locations of binding sites:

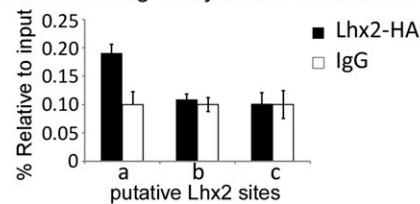
- a) chr10 106,987,527
- b) chr10 106,987,604
- c) chr10 107,004,375



D. Lhx2 and Myogenesis



Lhx2 binding to *Myf5* MAE in C2C12



E. *In vivo* ChIP for PM regulators

	<i>Myf5</i> (MAE)	<i>Myf5</i> neg. +10kb	<i>Myf5</i> neg. -40kb
α-Tbx1	++	-	-
α-Pitx2	+++	-	-
α-Tcf21	+++	-	-

+ weak; ++ moderate; +++ strong binding

Fig. S5. ChIP data. (A) ChIP for proximal promoters of PM regulators, using Tbx1, Pitx2, and Tcf21 antibodies. The gene expression shown by qRT-PCR is presented relative to the total input. (B) Additional Pitx2 binding sites on the *Tbx1* promoter. (C) Three putative Lhx2 binding sites on the *Myf5* mandibular arch enhancer (MAE). (D) Western blot and ChIP for *Myf5* MAE, using HA antibody and Lhx2-HA construct in vitro (D). (E) An *in vivo* ChIP experiment using pharyngeal arch tissues at E9.5 with Tbx1, Pitx2, and Tcf21 antibodies suggest a range of direct interactions with the *Myf5* MAE.

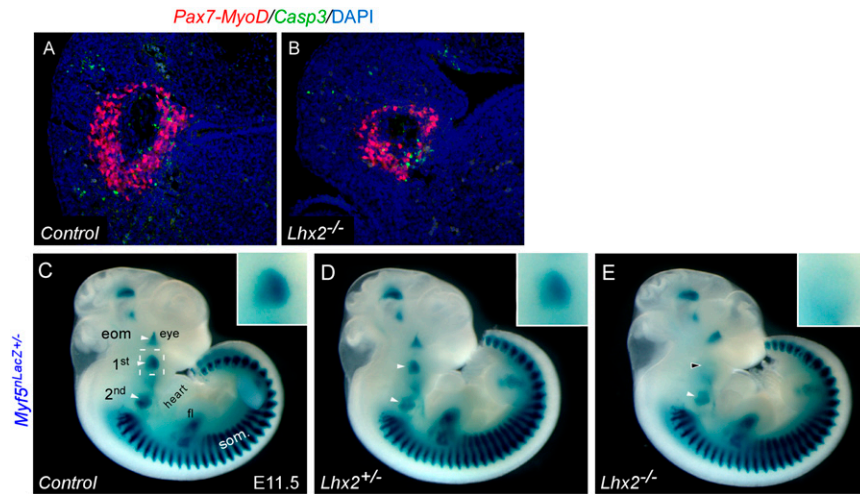


Fig. 56. Comparable apoptosis in the PM of controls and *Lhx2* mutants. (A and B) Transverse sections of control (A) and *Lhx2* mutant (B) E11.5 embryos, showing the core of the PM. Coimmunofluorescence of Pax7-MyoD and activated caspase3 (Casp3) cells in control (A) and *Lhx2* mutant (B) embryos. (C–E) *Myf5* expression (X-Gal staining) in *Lhx2* control (C), heterozygous (D) and homozygote (E) E11.5 embryos, which are also heterozygous for the *Myf5*^{nLacZ} reporter. (Insets) The area depicted by the dotted line in C. Arrowheads indicate change in muscle patterning. Eom, extraocular muscles; first/second, first/second pharyngeal arch muscle progenitors; fl, forelimb; som, somites.

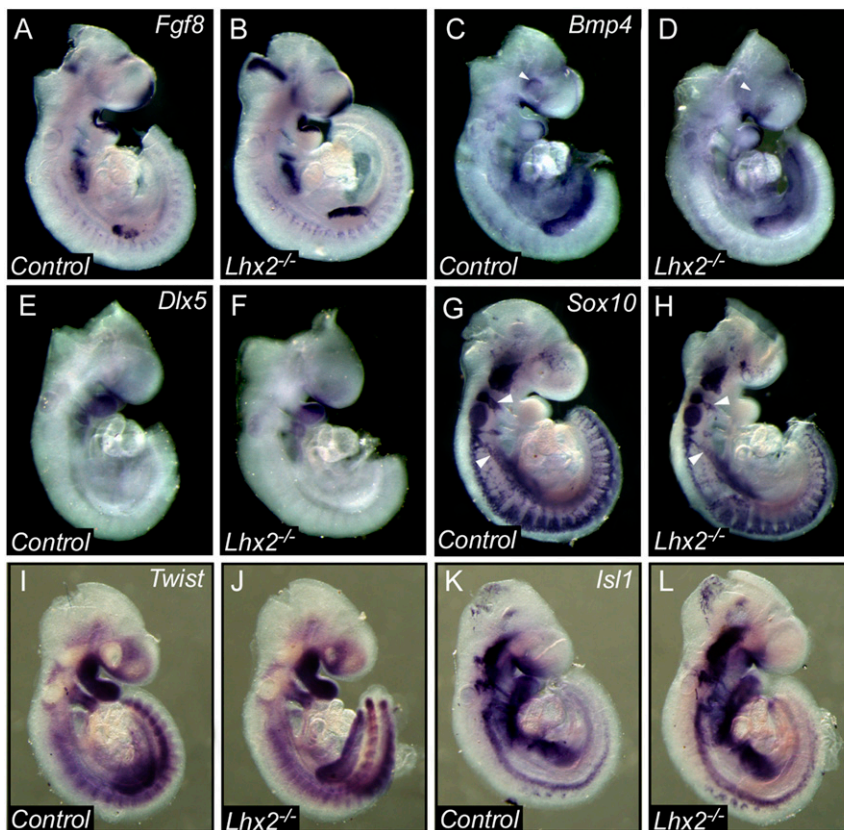


Fig. 57. In situ hybridization analysis for *Lhx2*^{-/-} embryos. Whole-mount in situ hybridization for in E9.5 embryos (*Lhx2*^{-/-} and controls) for *Fgf8* (A and B), *Bmp4* (C and D), *Dlx5* (E and F), *Sox10* (G and H), *Twist* (I and J), and *Isl1* (K and L). White arrowheads indicate down-regulation of *Bmp4* in the eye of *Lhx2*^{-/-} compared with controls (C and D) or defected neural crest migration in *Lhx2*^{-/-} compared with controls (G and H).

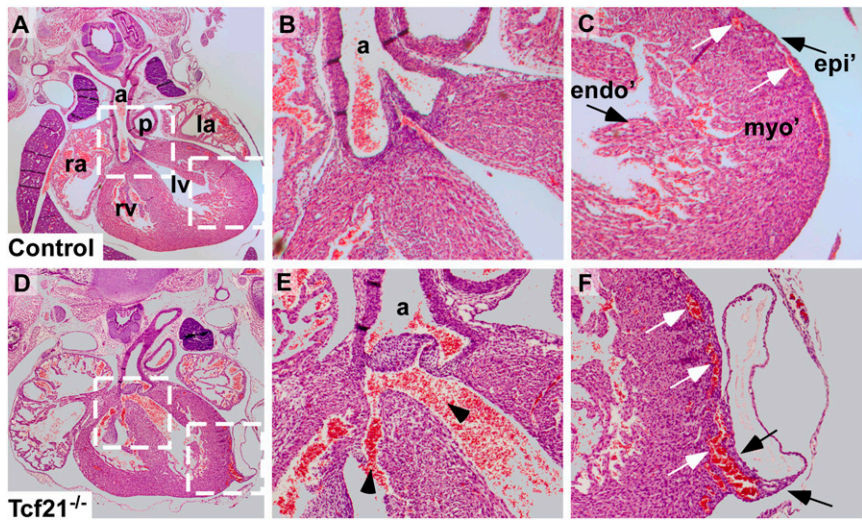


Fig. S8. Heart malformations in *Tcf21*^{-/-} embryos. (A–C) H&E staining of heart paraffin sections in control hearts (A) and enlarged insets (B and C). (D–F) *Tcf21*^{-/-} mutants display tetralogy of Fallot, characterized by both ventricular septal defect and overriding aorta (E, arrowheads), as well as detached epicardium and aberrant coronary vessels (F, white arrows) compared with the controls (C). a, aorta; endo', endocardium; epi', epicardium; la, left atrium; lv, left ventricle; myo', Myocardium; p, pulmonary artery; ra, right atrium; rv, right ventricle.

Table S1. Genotypes/phenotypes summary

Anomalies and defects	E17			E14.5				
	WT	<i>Lhx2</i> ^{mKO}	<i>Tcf21</i> ^{-/-}	<i>Lhx2</i> ^{-/-}	<i>Tbx1</i> ^{+/-}	<i>Tbx1</i> ^{+/-} <i>Lhx2</i> ^{+/-}	<i>Tbx1</i> ^{-/-}	<i>Tbx1</i> ^{-/-} <i>Lhx2</i> ^{-/-}
Craniofacial anomalies	0%	0%	100%	100%				
Cleft palate	0%	0%	100%	100%				
Cardiovascular defects	0%	50%	30%	N/A				
Tetralogy of Fallot	0%	30% (4/13)	30% (3/11)	N/A				
Persistent truncus arteriosus	0%	0%	0%	N/A				
Transposition of the great arteries	0%	0%	0%	N/A				
Ventricular septal defects	0%	7% (1/13)	0%	N/A	0%	20% (2/10)	100% (5/5)	100% (4/4)
Double-outlet right ventricle	0%	15% (2/13)		N/A				
Aortic arch anomalies	0%	0%	0%	0%				
Total	n = 10	n = 13	n = 11	n = 10	n = 11	n = 10	n = 5	n = 4

A table summarizing craniofacial, cardiovascular, and aortic arch defects in *Lhx2*^{mKO}, *Lhx2*^{null}, *Tcf21*^{null}, and control E17.5 embryos. Because ventricular septal defect was evident in all hearts of *Tbx1*^{-/-} (n = 5), we could not see differences in *Tbx1*^{-/-}*Lhx2*^{-/-} (n = 4) double mutants because of the saturation of this phenotype.

Table S2. List of primers

Fig. 5 panel	Forward primers	Reverse primers
Primers for Fig. 5A		
ChIP-qPCR		
Msc_prom	GGCCTAAGTCTTTGCTTTGC	TCCGGATCCAAAAGTACAGC
Tcf21_prom_F1	AAAGGGGCCTTAGGAGATGA	CGAGGAATTTGGTGGACT
Pitx2ab_prom	TCCTTGTCCTTTCTACCA	GGACCACTAGGGCTGAGAAG
Pitx2c_prom	TCTCCTCCTCCACCTTAT	AGGGATGGTTCTGTCTGCAC
Tbx1_prom	CGGAAGGGAAGACATGAAAA	ACGCTCCCAAGTTCTTCTT
Myf5 -40	CACCCAAGGCCATTACCG	GTTGTCCTCGGGCCAATACTG
Myf5 pro	AATGTCTTGCTACCGTGCTG	GGTCCCTTTGACGCTAATGA
Myf5 -10 kb	TCCTTCTCCCACTTTTCTGA	GACATGGCAACTGTGGAATG
Primers for Fig. 5B		
ChIP-qPCR		
Tbx1	TTATGCACCTGCCCAAGACT	GGCTGTCAAGAGGTCGTTTC
Tcf21	CAGCTCATGTAGGCATCTGG	CCGAGGATAAAGCAGGAGTG
Lhx2a	TGGCTTTGGTCTCAGAATCC	TCCTTTCTGCGGGTCTCTAA
Lhx2b	GGCCACATGGCTTTCCCAAT	TCTTCCACCCCTCCACACCTT
Lhx2c	TGGGTGGACATGCCCTTTCACCT	AGAGCCTCAAACCTCACTGTGGC
qPCR		
Lhx2	CCAGCTTCGGACAATGAAGT	TTTCCTGCCGTAAGAGTTG
Tbx1	GCTGTGGGACGAGTTCAATC	ACGTGGGGAACATTCTGCT
Tcf21	GGCTGGCGTCCAGCTACATCG	TGCCGGCCACCATAAAGGGC
Pitx2	TGGACCAACCTTACGGAAGC	GACAGAGACGTTGACGTGAGG